

where the energy stored in them will be used to drive the protons across the inner membrane and out of the mitochondria via respiration driven-proton pumps. Finally, the gradient of protons created by the pumps is harvested F_1F_0 -ATPase to phosphorylate ADP to produce ATP, the basic unit of energy exchange [45]. Stages 2 and 3 and the modeling efforts to describe them will be discussed below.

The TCA cycle (Figure 7) is the common mode of oxidative degradation in eukaryotes and prokaryotes and marks the “hub” of the metabolic system, accounting for the major portion of carbohydrate, fatty acid, and amino acid oxidation and generating numerous biosynthetic precursors. The eight enzymes of the cycle catalyze a series of well-known organic reactions that cumulatively oxidizes an acetyl group of acetyl-CoA to two CO_2 molecules with the concomitant generation of three NADHs, one FADH_2 , and one GTP.

Remarkably, despite the complexity of the internal processes, the TCA cycle maintains a steady state. Since there generally exist reactions that “commit” the intermediate to continue down the pathway, the most efficient way to exert control is to regulate the enzymes that catalyze these committed steps. However, these steps often function too slowly to achieve equilibrium of substrate and product while other reactions function closer to equilibrium. Therefore, in order to control the flux of metabolites through the pathways, it is important to exert control here, since further extraneous metabolite synthesis can be avoided. The establishment of these steps is difficult, however, because

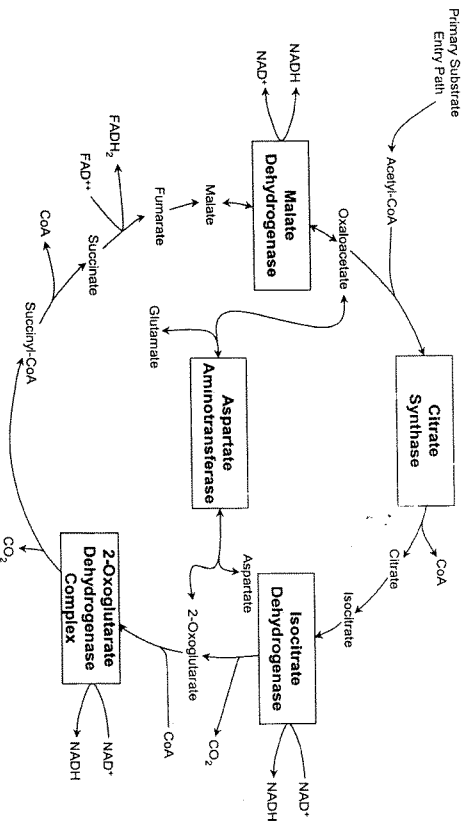


Figure 7. Schematic diagram of the tricarboxylic acid cycle. The regulatory enzymes (shown in boxes) were modeled in detail in the Dudycha-Iatiri model of the TCA cycle.

most of the cycle's metabolites are present in both mitochondria and cytosol. Plus, the distribution between the two compartments is not known in order to determine ΔG of each reaction from the concentrations of the substrates and products. However, when equilibrium of distribution is assumed, the total cell contents of the substances can be used to estimate the mitochondrial concentrations. After evaluation of the ΔG s, only three enzymes are likely to function at a significant deviation from the equilibrium under physiological condition: citrate synthase, isocitrate dehydrogenase, and α -ketoglutarate dehydrogenase [45]. Therefore, they are considered as our rate-controlling enzymes. The regulatory enzymes here seem to be controlled almost entirely by substrate availability, product inhibition, and competitive feedback inhibition by other intermediates further along the cycle as well as allosteric regulators such as Ca^{2+} and H^+ [45].

Modeling cardiac energy metabolism

Currently, our research is aimed towards investigating the mechanisms of mitochondrial respiration through the completion of a physiologically verifiable mitochondrial model, which can simulate the regulation of respiration through the fluctuation of Ca^{2+} , NADH, ADP, and pH levels to date. To this end, a detailed model of the TCA cycle has been developed based on experimental findings. The TCA cycle model has been coupled with a mitochondrial model that included electron transport and ATP synthesis to create a model of mitochondrial energy metabolism.

The Dudycha-Iafri model of the TCA cycle [51, 52] uses a reversible Michaelis-Menten formalism to describe the key regulatory enzymes, namely, citrate synthase, isocitrate dehydrogenase, α -ketoglutarate dehydrogenase, and malate dehydrogenase. These are shown in boxes in Figure 7. Also shown in a box is aspartate aminotransferase, which can have potent effects on TCA cycle function. The data from *in vitro* studies of isolate enzymes has been used to determine the dependence of the enzymes on various regulatory factors. A simultaneous fit for the equations to all the experimental data has been performed. The results were remarkably good given the fact that the measurements of enzyme activities came from different labs using different preparations. Details of those descriptions follow.

The enzyme citrate synthase catalyzes the condensation of acetyl-CoA and oxaloacetate to mark the initial TCA reaction. This mixed aldol-Claisen ester condensation reaction proceeds with a sequential kinetic mechanism, with oxaloacetate binding to the enzyme to conformationally generate a binding site for acetyl-CoA.

$$V_{CS} = \frac{k_f [E]_t}{1 + \frac{K_{M,A-CoA}}{[A-CoA]} + \frac{K_{M,OxM}}{[OxM]} \left(1 + \frac{[A-CoA]}{K_{i,A-CoA}} \right) + \frac{K_{S,A-CoA}}{[A-CoA]} \frac{K_{M,OxM}}{[OxM]}}$$

An interesting result of this model is that in order to fit the experimental data, substrate inhibition by acetyl-CoA must be present.

Isoctrate dehydrogenase catalyzes the oxidative decarboxylation of isocitrate to α -ketoglutarate to produce TCA's 1st CO₂ and NADH. This NAD⁺-dependent enzyme requires an Mn²⁺ or Mg²⁺ as a cofactor.

$$\begin{aligned}
 v_{IHD} &= \frac{k_{cat}[E]_I}{f_h + \left(\frac{K_{M,ISOC}}{[ISOC]} \right)^{n_{hox}} + \left(\frac{K_{M,NAD^+}}{[NAD^+]} \right)^{n_{hdo}} f_i + \frac{\left(\frac{K_{M,ISOC}}{[ISOC]} \right)^{n_{hox}} \left(\frac{K_{M,NAD^+}}{[NAD^+]} \right)^{n_{hdo}}}{f_u}} \\
 f_h &= \left(1 + \frac{[H]}{K_{h1}} + \frac{K_{h2}}{[H]} \right) \\
 f_h &= \left(1 + \frac{[ADP]}{K_{u,ADP}} \right) \left(1 + \frac{[Ca^{2+}]}{K_{ca^{2+}}} \right) \\
 f_i &= \left(1 + \frac{[NADH]}{K_{i,NADH}} \right)
 \end{aligned}$$

The α -ketoglutarate dehydrogenase complex (KGDHC), a homologous 3-enzyme complex, functions to catalyze the oxidative decarboxylation of an α -keto acid, releasing a TCA cycle's 2nd CO₂ and NADH. Its components include α -ketoglutarate dehydrogenase (E₁), dihydrolipoyl transsuccinylase (E₂), and dihydrolipoyl dehydrogenase (E₃). Each component catalyzes a separate reaction. However, the overall reaction can be modeled by the equation

$$v_{KODHC} = \frac{k_{cat}[E]_I}{1 + \left(\frac{K_{M,adG}}{\alpha KG} \right)^{n_{ad}} + \left(\frac{K_{M,NAD}}{NAD^+} \right)^{n_{hdo}} \left(1 + \frac{Mg}{K_{d,Mg}} \right) \left(1 + \frac{Ca}{K_{d,Ca}} \right)}$$

Malate dehydrogenase catalyzes the final TCA reaction to regenerate oxaloacetate, oxidizing malate's hydroxyl group to a ketone in a NAD⁺-dependent reaction. The result is the production of another NADH molecule.

$$v_{NADH} = \frac{k_r \cdot f_h \cdot [E]_t}{1 + \frac{K_{M,MAL}}{[MAL]} \left(1 + \frac{[OAA]}{K_{i,OAA}} \right) + \frac{K_{M,NAD^+}}{[NAD^+]} + \frac{K_{M,MAL}}{[MAL]} \left(1 + \frac{[OAA]}{K_{i,OAA}} \right) \frac{K_{S,NAD^+}}{[NAD^+]}}$$

$$f_h = f_{h,i} \cdot f_{h,a}$$

$$f_{h,a} = \frac{1}{1 + \frac{[H^+]}{K_{h,1}} + \frac{[H^+]^2}{K_{h,1}K_{h,2}}} + k_{offset}$$

$$f_{h,i} = \left(\frac{1}{1 + \frac{K_{h,3}}{[H^+]} + \frac{K_{h,3}K_{h,4}}{[H^+]^2}} \right)^2$$

The remaining TCA cycle enzymes are described using the law of mass action. In order to get an accurate estimate of total cycle flux, the contributions of the individual enzymes to the TCA cycle flux are optimized to conform to the TCA cycle flux experiments measuring ^{13}C enrichment studies using NMR. The cycle produces fluxes and substrate intermediate concentrations consistent with experimentally determined values. The model is then used to study the effects of mitochondrial pH, redox ratio $([\text{NADH}]/[\text{NAD}^+])$, $[\text{ADP}]$, and $[\text{Ca}^{2+}]$.

Figure 8 shows the dependence of the TCA cycle flux as measured by NADH production on mitochondrial pH, redox ratio, and $[\text{Ca}^{2+}]$. The NADH production flux shows a dome shaped pH dependence with the peak being almost flat between pH values of 7.0 and 7.4 which are the physiologically relevant value for healthy mitochondria. Notice that as pH drops below 7.0 (as would be the case during ischemia), the efficiency of NADH production declines (Figure 8A). The NADH production falls rapidly as the redox ratio increases and then plateaus. This suggests a homeostatic mechanism such that as NADH levels rises, it produces a negative feedback on the TCA cycle, reducing the production of NADH (Figure 8B). When ADP increases, the NADH production increases and then plateaus such that in the physiological ranges of $[\text{ADP}]$, the curve is almost flat (Figure 8C). This suggests that $[\text{ADP}]$ is not a potent regulator of TCA cycle flux. As $[\text{Ca}^{2+}]$ rises, the NADH production flux rises and then plateaus (Figure 8D). However, for physiological mitochondrial $[\text{Ca}^{2+}]$, the curve is relatively steep, indicating that Ca^{2+} is a potent regulator of the TCA cycle.

The TCA cycle model is then coupled with the Magnus-Keizer mitochondrial model [53] that describes Ca^{2+} handling and ion transport,

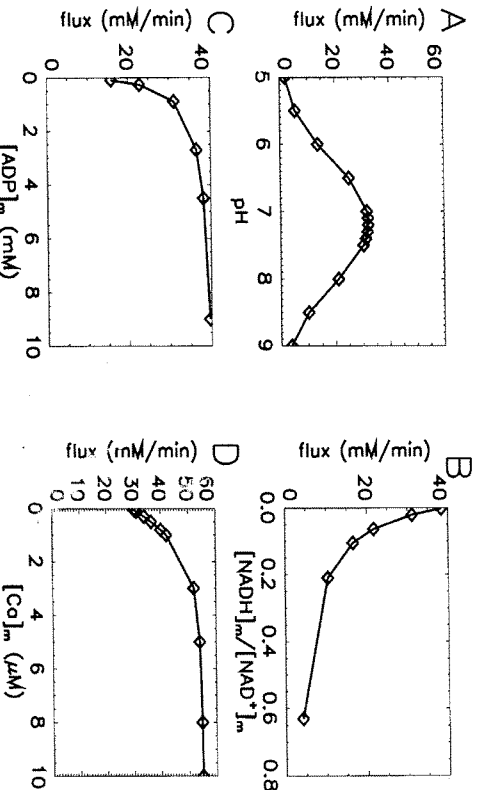


Figure 8. Simulations of the regulation of the TCA cycle using the Dudycha-Jafri model with respect to changes in A. mitochondrial pH. B. redox potential ($[NADH]_m/[NAD^+]_m$). C. $[ADP]_m$. D. $[Ca^{2+}]_m$

verified by simulating isolated mitochondrial responses to brief pulses of Ca^{2+} . In this model, there exist six methods of ion transport. These include the proton pump via respiration (which produces the gradient for ATP synthesis), proton uptake by F_1F_0 -ATPase, proton leak, adenine nucleotide translocase, $NaCa$ exchanger, and the Ca^{2+} uniporter. Two significant findings for the model are as follows: 1) parallel activation by Ca^{2+} is necessary to see any effective activating effect by Ca^{2+} and 2) the NADH levels are very well regulated. These are described in detail below.

Generally, cytosolic Ca^{2+} is regarded as a significant regulatory signal for oxidative metabolism in the mitochondria, the main pathway where energy is converted to ATP. Through the literature, it has been suggested that both ATP consumption by ATPases involved in ionic homeostasis and myofibril contraction as well as ATP production by the mitochondria is regulated by Ca^{2+} in a parallel activation scheme [54]. It also has been suggested that there is parallel activation of mitochondrial energy production, i.e. Ca^{2+} serves to activate the F_1F_0 -ATPase and the TCA cycle simultaneously [46]. In fact, Balaban and his research group investigated the role of cytosolic Ca^{2+} as a signal for activation of mitochondrial ATP production. Their measurements show that Ca^{2+} induces as much as a 5-fold increase in ATP production, while statistically insignificant changes in mitochondrial NADH levels are observed [46].

Furthermore, it is suggested by Territo and co-workers that >60% of Ca^{2+} activation occurs downstream of the TCA cycle [49].

The model demonstrates the parallel activation of mitochondrial energy production nicely. When activation of the F_1F_0 -ATPase is not included, increases in Ca^{2+} do not effectively increase ATP production (Figure 9A; gray trace). However, when the Ca^{2+} dependence as measured by Balaban and co-workers [46] is included, increases in Ca^{2+} effectively increase ATP production (Figure 9A; black trace). Another interesting prediction of the model that is supported by the experimental data [46] is that with parallel activation, even while the ATP production rate rises in response to increasing Ca^{2+} , the $[\text{NADH}]$ remains relatively constant (Figure 9B; black trace). However, when Ca^{2+} activation of the F_1F_0 -ATPase is not included, the NADH levels rise in response

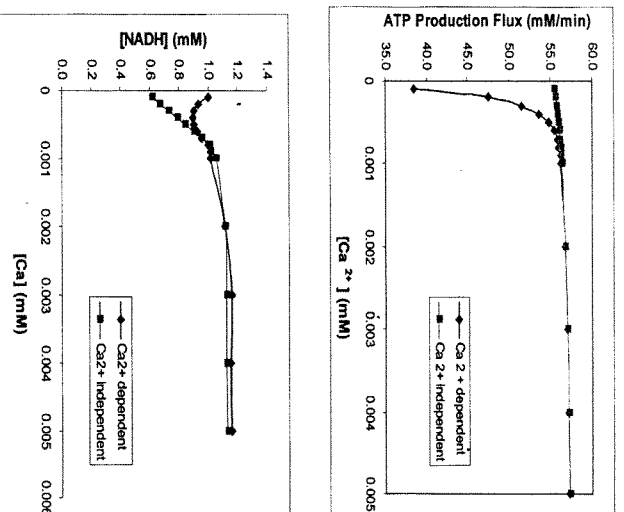


Figure 9. Simulations with the Nguyen-Jafri model for mitochondrial energy metabolism. A. $[\text{Ca}^{2+}]$ fails to activate mitochondrial energy metabolism if only the TCA cycle is activated by Ca^{2+} (gray). $[\text{Ca}^{2+}]$ activates mitochondrial energy metabolism when both the TCA cycle and the F_1F_0 -ATPase (black) are activated by Ca^{2+} . B. $[\text{NADH}]$ increases with increasing Ca^{2+} if only the TCA cycle is activated by Ca^{2+} (gray). When both the TCA cycle and the F_1F_0 -ATPase are activated by Ca^{2+} (black), $[\text{NADH}]$ remains relatively constant.

to increasing Ca^{2+} (Figure 9B; gray trace). This results because with Ca^{2+} activation of the TCA cycle, [NADH] production is increased while its consumption does not. The rising [NADH] inhibits the TCA cycle, reducing the steady-state rise in flux through the cycle.

Conclusions

Computational modeling has proven to be a valuable area of study to gain insight in the complex mechanisms governing the function of the heart. This manuscript has described a number of modeling efforts by and the predictions that have been made through these efforts in the areas of excitation-contraction coupling and energy metabolism. However, it is important to note that there are many other contributions computational modeling has provided that are not described here due to space limitations.

To summarize some of the contributions described in this manuscript, the can be classified into two broad categories. The first is the modeling give insights in to mechanisms that are responsible for experimentally observation in complex systems. These insights can be the basis of predictions and new hypothesis that can be tested experimentally. In this light, it is important to make these predictions in an experimentally verifiable manner. Examples of this include, the predictions of the importance of the L-type Ca^{2+} current on determining action potential shape and duration or the importance of the SERCA pumps in determining force-frequency relations. Second, the modeling can be used to make predictions and for hypotheses about mechanisms that are beyond our ability to measure. Often, there exists a set of experimental data, and the modeling can be used to see if the collection and integration of this data can explain what is experimentally observable. This is exemplified by the work done in the dyadic space to study graded release or the mechanism of Ca^{2+} sparks.

It is likely, that computational modeling will continue to increase in importance as a tool to gain insight into the cellular and subcellular systems that govern cellular function in the cardiac myocyte and other systems. As modeling tools make modeling more accessible to a wider audience, the use of models will increase. Also as the amount of detailed experimental data increases, it will become increasingly necessary to use the computational model to integrate the data to understand living systems.

References

1. Berridge, M., Bootman, M. and Lipp, P., 1998, *Nature*, 395, 645-648
2. Marban, E., 2002, *Nature*, 415, 213-218
3. Bers, D. M., *Excitation-Contraction Coupling and Cardiac Contractile Force*, Kluwer
4. Linz, K. W. and Meyer, R., 2000, *Pflügers Arch - Eur J Physiol*, 439, 588-599

5. Fbiato, A. J. G., 1985, *J. Gen Physiol*, 85, 247-289
6. Cheng, H., Lederer, W. J. and Cannell, M. B., 1993, *Science*, 262, 740-744
7. Cheng, H., Lederer, M. R., Xiao, R. P., Gomez, A. M., Zhou, Y. Y., Ziman, B., Spurgeon, H., Lakatta, E. G. and Lederer, W. J., 1996, *Cell Calcium*, 20, 129-140
8. Gauthiostom, S., Dilly, K., Santana, L. F., Jafri, M. S., Sobie, E. A. and Lederer, W. J., 2002, *J Mol Cell Cardiol*, 34, 941-950
9. Williams, A. J., 1997, *Eur. Heart J*, 18, A27-A35
10. DiFrancesco, D. and Noble, D., 1985, *Philosophical Transactions of Royal Society, B* 307,
11. Luo, C. H. and Rudy, Y., 1994, *Circulation Research*, 74, 1071-1096
12. Luo, C. H. and Rudy, Y., 1994, *Circulation Research*, 74, 1097-1113
13. Jafri, M. S., Rice, J. J. and Winslow, R. L., 1998, *Biophysical Journal*, 74, 1149-1168
14. Winslow, R. L., Rice, J. J., Jafri, M. S., Marban, E. and O'Rourke, B., 1999, *Circ Res*, 84, 571-586
15. Rice, J. J., Jafri, M. S. and Winslow, R. L., 2000, *Am J Physiol Heart Circ Physiol*, 278, H913 H931
16. Keizer, J. and Levine, L., 1996, *Biophysical Journal*, 6, 3477-3487
17. Lee, K. S., Marban, E. and T sien, R. W., 1985, *Journal of Physiology*, 364, 395-411
18. Yue, D. T. and Marban, E., 1990, *J Gen Physiol*, 95, 911-939
19. Imredy, J. P. and Yue, D. T., 1994, *Neuron*, 12, 1301-1318
20. Gyorko, I. and S.Gyorko, 1998, *Biophysical Journal*, 75, 2801-2810
21. Santana, L. F., Cheng, H., Gomez, A. M., Cannell, M. B. and Lederer, W. J., 1996, *Circulation Research*, 78, 166-171
22. Isenberg, G. (1995) in *Physiology and Pathophysiology of the Heart: Developments in Cardiovascular Medicine*, vol. 151, pp. 289-307, Kluwer, Boston
23. Cannell, M. B., Cheng, H. and Lederer, W. J., 1994, *Biophysical Journal*, 67, 1942-1956
24. Rice, J. J., Jafri, M. S. and Winslow, R. L., 1999, *Biophys J*, 77, 1871-84
25. Rice, J. J., Winslow, R. L. and Hunter, W. C., 1999, *Am J Physiol*, 276, H1734-54
26. Runberger, E. and Timmermann, J., 1976, *Eur J Appl Physiol Occup Physiol*, 35, 277-84
27. Huke, S., Liu, L. H., Biniakiewicz, D., Abraham, W. T. and Periasamy, M., 2003, *Cardiovasc Res*, 59, 668-77
28. Muller, O. J., Lange, M., Rattunde, H., Lorenzen, H. P., Muller, M., Frey, N., Bitter, C., Simonides, W., Katus, H. A. and Franz, W. M., 2003, *Cardiovasc Res*, 59, 380-389
29. Linz, K. W. and Meyer, R., 1998, *Journal of Physiology*, 513, 425-442
30. Stern, M. D., 1992, *Biophysical Journal*, 63, 497-517
31. Stern, M. D., Song, L.-S., Cheng, H., Sham, J. S. K., Yang, H. T., Boheler, K. R. and Rios, E., 1999, *J Gen Physiol*, 113, 469-89
32. Valdivia, H., Kaplan, J., Ellis-Davies, G. and WJ, L., 1995, *Science*, 267, 1997-2000
33. Beuckelmann, D. J., Nabauer, M. and Erdmann, E., 1993, *circ res*, 73, 379-385
34. Lima, C. J., Olivari, M.-T., Goldenberry, I. F., Levine, T. B., Benditt, D. G. and Simon, A., 1987, *Cardiovasc Res*, 21, 601-605

35. Reinecke, H., Studer, R., Vetter, R., Holz, J. and Drexler, H., 1996, *Cardiovasc Res*, 31, 48-54
36. O'Rourke, B., Kass, D. A., Tomaselli, G. F., Kääh, S., Tunin, R. and Marbán, E., 1999, *Circ. Res.*, 84, 562-570
37. Beuckelmann, D. J. and Wier, W. G., 1988, *Journal of Physiology*, 405, 233-255
38. Sobie, E. A., Dilly, K. W., Cruz, J. d. S., Lederer, W. J. and Jafri, M. S., 2002, *Biophysical Journal*, 37408,
39. Marx, S. O., Gaburjakova, J., Gaburjakova, M., Henrikson, C., Ondrias, K. and Marks, A. R., 2001, *Circ Res*, 88, 1151-8
40. Lehnart, S. E., Huang, F., Marx, S. O. and Marks, A. R., 2003, *Curr Top Med Chem*, 3, 1383-91
41. Ima, G., Nichole, H., Larry R., J. and Sandor, G., 2004, *Biophysical Journal*, 86, 2121-2128
42. Wang, J., N. A., Maertz, A. J., Lokuta, E. G., Kranias and Valdivia, H. H., 2001, *Biophysical Journal*, 80, 590a
43. Snyder, S. M., Palmer, B. M. and Moore, R. L., 2000, *Biophysical Journal*, 79, 94-115
44. Smith, G. D., Keizer, J. E., Stern, M. D., Lederer, W. J. and Cheng, H., 1998, *Biophysical Journal*, 75, 15-32
45. Jafri, M. S., Dudycha, S. J. and O'Rourke, B., 2001, *Annu Rev Biomed Eng.*, 3, 57-81
46. Balaban, R. S., Bose, S., French, S. and Territo, P. R., 2003, *Am J Physiol Cell Physiol*, 278, C285-C293
47. Bose, S., French, S., Evans, F. J., Joubert, F. and Balaban, R. S., 2003, *J Bio Chem*, 278, 39155-39165
48. McCormack, J. G. and Denton, R. M., 1993, *Dev Neurosci*, 15, 165-73
49. Territo, P. R., Mootha, V. K., French, S. A. and Balaban, R. S., 2000, *Am J Physiol Cell Physiol*, 278, C423-C435
50. Neely, J. R. and Morgan, H. E., 1974, *Annu Rev Physiol*, 36, 413-459
51. Dudycha, S. J. (2000) in *Department of Biomedical Engineering, The Johns Hopkins University School of Medicine, Baltimore*
52. Dudycha, S. and Jafri, M. S., 2001, *Biophys J*, 80, 589
53. Keizer, G. M. a. J., 1997, *Am J Physiol*, 42, C717-C733
54. Korzeniewski, B. and Mazat, J.-P., 1996, *Biochem. J.*, 319, 143-48

